Crossing-consistent analysis of kaon photoproduction and radiative capture

Robert Williams, Chueng-Ryong Ji, and Stephen R. Cotanch
Department of Physics, North Carolina State University, Raleigh, North Carolina 27695-8202
(Received 2 March 1989; revised manuscript received 22 January 1990)

A crossing-consistent description is presented for K^+ photoproduction $p(\gamma,K^+)\Lambda$ and K^- radiative capture $p(K^-,\gamma)\Lambda$ using an effective-chiral-Lagrangian model. Crossing requires that these reactions should both be described by the same physical model including identical dynamic parameters such as coupling constants. It is demonstrated that previous analyses of these crossing-related reactions, which have also used this effective-chiral-Lagrangian model, have not utilized the crossing constraint and thus do not simultaneously describe both kaon photoproduction and capture. New sets of coupling constants that consistently describe both reactions are presented.

I. INTRODUCTION

"Effective" hadronic field theories, such as quantum hadrodynamics[1] (QHD), have no explicit quark degrees of freedom but can be used to describe phenomenologically intermediate- and low-energy particle reactions. QHD is properly relativistic and is naturally suited to the diagrammatic covariant S-matrix formalism. The theory presupposes the existence of strong-coupling parameters which can be phenomenologically determined. Previous researchers have separately investigated the crossing-related kaon photoproduction $p(\gamma,K^+)\Lambda$ and capture $p(K^-,\gamma)\Lambda$ reactions within the QHD framework and have obtained a number of possible strong-coupling parametrizations.[2–6] However, no study to date has incorporated the crossing symmetry of the analytic S matrix to simultaneously analyze both reactions.

Crossing is believed to be an exact symmetry, based on the *CPT* theorem and analyticity of the S matrix.[7] Crossing-related reactions, such as kaon photoproduction and radiative capture, are described by the same transition amplitude evaluated in different kinematic regions of the S matrix. Even if the model uses running coupling constants, this statement should be correct when the magnitude of momentum transfer involved in crossed reactions is the same. As an example, the same form of quantum-chromodynamic coupling constant $\alpha_s(|q^2|)$ can be used both in timelike and spacelike regions of q^2. For QHD phenomenological analyses,[2–4] previous investigations have demonstrated that a reasonable description of low-energy kaon photoproduction is possible using energy-independent coupling constants over a relatively large energy range, roughly 500 MeV from threshold to 1.4 GeV. Since this analysis is restricted to K^+ photoproduction energies below 1.4 GeV and because the maximum c.m. energy difference between K^-p capture at rest and K^+ photoproduction is also less than 500 MeV, it is reasonable to expect that both reactions should be described by the same energy-independent coupling constants. The purpose of this paper is to report a new, improved analysis which, by respecting the crossing constraint, has obtained consistent strong-coupling parametrizations which simultaneously describe both kaon photoproduction and capture processes.

This paper is organized into four sections. Section II contains formalism and the details of our calculations. Our results are presented in Sec. III where numerical computations of cross sections, branching ratios, and polarizations, using the parametrizations we have found, provide a good description of available data for both reactions considered. Also, the sensitivity to uncertainties in model parameters is documented. Because this sensitivity is channel dependent, different parametrizations that fit data for a reaction in one channel will produce very different cross-channel predictions; hence crossing can be used to eliminate the "unphysical" model parametrizations. We summarize and further discuss our results in Sec. IV.

II. FORMALISM AND MODEL DETAILS

We investigated the specific QHD model parametrizations of Refs. 2, 3, 4, and 5 [hereafter we designate these PR2, PR3(a,b), PR4(a,b), and PR5, respectively] for the sake of comparison. We denote the parameter sets which we have found by C1 and C2. A "model" (here) is defined to be a specific set of pole-model resonances which are believed to make significant contributions to the transition amplitude. Discussion about a specific model can be found in the paper of the corresponding reference. For notation, we define the five models considered in this paper as follows:

$$\{\text{Born}\}=\{\Lambda,\Sigma,K,K^*\}\ ,$$

$$\text{M1}=\{\text{Born}\}\ ,$$

$$\text{M2}=\{\text{Born},N_1,N_4\}\ ,$$

$$\text{M3}=\{\text{Born},Y_1,Y_2,Y_3,N_4,N_6\}\ ,$$

$$\text{M4}=\{\text{Born},K_1,Y_2,N_1,N_4\}\ ,$$

$$\text{M5}=\{\text{M3},N_1,K_1\}\ ,$$

where we have used the standard notation for identifying specific Y^*, N^*, and K^* resonances (masses and widths for the various states are listed in Table I). Model M5 is unique to this analysis where we simultaneously consider

TABLE I. Masses and widths of various states used in our models.

Particle	J^P	Mass (GeV)	Width (GeV)
p	$\frac{1}{2}^+$	0.938 28	
K^+	0^-	0.493 67	
K^{*+}	1^-	0.892 10	0.051
Λ	$\frac{1}{2}^+$	1.115 60	
Σ	$\frac{1}{2}^+$	1.192 46	
Y_1	$\frac{1}{2}^-$	1.405	0.04
Y_2	$\frac{1}{2}^-$	1.670	0.040
Y_3	$\frac{1}{2}^-$	1.800	0.300
N_1	$\frac{1}{2}^+$	1.470	0.200
N_4	$\frac{1}{2}^-$	1.650	0.150
N_6	$\frac{1}{2}^+$	1.710	0.120
$K1$	1^+	1.280	0.090

all the diagrams of the other models.

Predictions for the experimental observables (cross sections, branching ratios, and polarizations) are calculated by standard theoretical expressions involving the transition amplitude. For clarity of discussion, selected details of the calculation are briefly summarized. Complete details can be found in Ref. 7.

The Lorentz-invariant transition amplitude T_{fi} has the same crossing properties as the S matrix, and is related by

$$S_{fi}=(\rho_a\rho_b\rho_c\rho_d)^{1/2}\delta_{fi}+i(2\pi)^4\delta(P_f-P_i)T_{fi} , \quad (1)$$

where a,b,c,d label the particles in the general two-body reaction

$$a+b\rightarrow c+d$$

and δ_{fi} contains Dirac and Krönecker δ functions representing the preservation of the initial state when no interaction occurs, with coefficients (ρ's) determined by the covariant normalization for single-particle states and with final and initial four-momenta labeled by P_f and P_i, respectively, (see Ref. 7 for details). For the reaction $p(\gamma,K^+)\Lambda$, the transition amplitude can be written as an expansion in terms of four Lorentz- and gauge-invariant amplitudes (A_j) and bilinear covariant matrices (M_j). The matrices are given by

$$\begin{aligned} M_1&=-\gamma_5\not{\epsilon}\not{P}_\gamma , \\ M_2&=2\gamma(\epsilon\cdot P_p P_\gamma\cdot P_\Lambda-\epsilon\cdot P_\Lambda P_\gamma\cdot P_p) , \\ M_3&=\gamma_5(\not{\epsilon}P_\gamma\cdot P_p-\not{P}_\gamma\epsilon\cdot P_p) , \\ M_4&=\gamma_5(\not{\epsilon}P_\gamma\cdot P_\Lambda-\not{P}_\gamma\epsilon\cdot P_\Lambda) , \end{aligned} \quad (2)$$

and the invariant elementary amplitudes are determined diagramatically from the Feynman rules. Propagators and vertex factors are well known and are listed in many sources (see Ref. 3).

In order to calculate branching ratios we use the kaonic atom approximation of Ref. 5 (zero kaon momentum, s-state capture). The branching-ratio result in our notation (in the c.m. frame) is given by

$$B=\frac{\Gamma_{K^-p\rightarrow\gamma\Lambda}}{\Gamma_{K^-p\rightarrow\text{all}}}=-\frac{k\left[\sum_{i,j=1}^{4}A_1^u A_j^u Q_{ij}^u\right]}{16\pi(m_K+m_p)m_K m_p W_p} , \quad (3)$$

where k is the c.m. photon energy, m_k and m_p are the kaon and proton mass, respectively, the Q matrix elements are functions of invariant Mandelstam variables s,t,u (listed in Table III below), and the u-channel amplitudes (A^u) are related to the s-channel amplitudes (A^s) through the crossing relations:

$$\begin{aligned} A_j^u(s,t,u)&=-A_j^s(u,t,s) , \\ Q_{ij}^u(s,t,u)&=Q_{ij}^s(u,t,s) . \end{aligned} \quad (4)$$

Also, W_p is the imaginary part of the K^-p pseudopotential (with the value 560 ± 135 MeV fm^3) used by Burkhardt, Lowe, and Rosenthal[8] to calculate the total decay rate for the capture process. After we used Eq. (4), we confirmed that the transition amplitude for the photoproduction process reproduces the amplitude for the kaon capture process presented in Ref. 5.

The polarization of the final-state Λ baryon is defined in the usual way as the asymmetry in the angular distributions between spin-up and spin-down Λ particles [here "up" is taken to be perpendicular to the production plane ($\mathbf{p}_\Lambda\times\mathbf{k}$)]:

$$\mathcal{P}_\Lambda=\frac{\left[\frac{d\sigma}{d\Omega}(\uparrow)-\frac{d\sigma}{d\Omega}(\downarrow)\right]}{\left[\frac{d\sigma}{d\Omega}(\uparrow)+\frac{d\sigma}{d\Omega}(\downarrow)\right]} . \quad (5)$$

Polarized cross sections are governed by the imaginary part of the amplitude and are related to the unpolarized cross section by

$$\frac{d\sigma}{d\Omega}(\uparrow,\downarrow)=\left.\frac{d\sigma}{d\Omega}\right|_{\text{unpol}} \mp\frac{|\mathbf{p}_\Lambda|^2\sin\theta_{\text{c.m.}}}{8\pi^2\sqrt{s}}\sum_{i,j=1}^{4}\text{Im}(A_i A_j^*)\text{Im}Q_{ij} , \quad (6)$$

where the minus sign is associated with spin up.

Using the pseudoscalar coupling scheme, we evaluated the Feynman diagrams (see Fig. 1) corresponding to the standard Born terms and the spin-$\frac{1}{2}$ resonances considered by Refs. 2–5. The resulting invariant amplitudes (A_j) are listed in the Appendix. To describe all models, there are a total of 12 effective parameters appearing in the amplitudes (any particular model may have less), four due to the Born terms and the rest coming from resonance contributions:

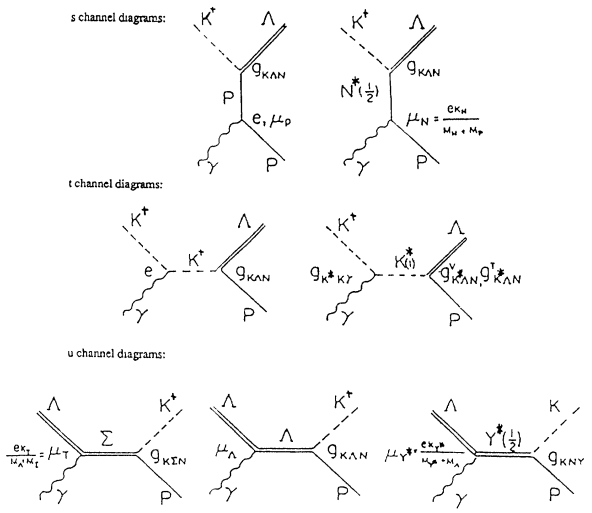

FIG. 1. Feynman diagrams for $p(\gamma,K^+)\Lambda$.

$$
\begin{aligned}
&g_\Lambda = g_{K\Lambda N},\quad G_{Y_1} = \kappa_{Y_1} g_{KNY_1}\ ,\\
&G_{N_1} = \kappa_{N_1} g_{K\Lambda N_1},\quad G_V^{K_1} = g_{K\gamma K_1} g_{K_1\Lambda N}^{V}\ ,\\
&G_\Sigma = \kappa_T g_{K\Sigma N},\quad G_{Y_2} = \kappa_{Y_2} g_{KNY_2}\ ,\\
&G_{N_4} = \kappa_{N_4} g_{K\Lambda N_4},\quad G_T^{K_1} = g_{K\gamma K_1} g_{K_1\Lambda N}^{T}\ ,\\
&G_V = g_{K^*K_\gamma} g_{K^*\Lambda N}^{V},\quad G_{Y_3} = \kappa_{Y_3} g_{KNY_3}\ ,\\
&G_{N_6} = \kappa_{N_6} g_{K\Lambda N_6},\quad G_T = g_{K^*K\gamma} g_{K^*\Lambda N}^{T}\ ,
\end{aligned}
\tag{7}
$$

involving products of the strong couplings g_{ABC}, the electromagnetic coupling $g_{AB\gamma}$ (where A,B,C are hadrons) and transition moments (κ's). We assume that the above resonances are sufficient for a proper dynamic analysis.

III. NUMERICAL ANALYSIS

We checked the validity of our branching ratio computation by reproducing all theoretical branching ratios (using the pseudoscalar coupling scheme) reported in Ref. 5. We also tested our K^+ production cross section and polarization calculation by reproducing the previous results

TABLE II. Couplings, predicted branching ratios, and χ^2 per point for the parametrizations considered.

Model	M1		M2	M3		M4	M5	
Parameter set	PR2	PR3a	PR3b	PR4a	PR4b	PR5	C1	C2
g_Λ	9.110	7.232	3.651	11.166	15.243	−13.187	7.434	10.581
G_Σ	5.388	−4.396	−2.861	11.627	12.762	11.812	−7.212	11.590
G_V	1.319	3.104	2.765	0.339	1.558	−1.147	3.869	0.323
G_T	0.804	−2.375	−0.603	−2.362	−4.247	−4.218	−4.116	−1.791
$G_V^{K_1}$				1.659	3.380		−0.211	1.986
$G_T^{K_1}$				0.792	10.418		−0.248	0.364
G_{Y_1}						−1.7	0.138	1.862
G_{Y_2}				2.474	11.875	0.059	0.169	−1.503
G_{Y_3}						0.255	0.704	0.703
G_{N_1}			5.211	−3.935	−3.215		−0.185	−2.104
G_{N_4}			0.358	0.358	0.365	0.358	0.112	0.273
G_{N_6}							0.101	0.037
s channel $p(\gamma,K^+)\Lambda$								
χ^2_σ	19.7	12.1	10.4	5.1	5.8	1.5×10^4	12.8	8.7
χ^2_σ(1.2 GeV)	13.9	3.42	3.2	3.7	3.9	9.5×10^3	0.7	3.4
$\chi^2_{\vec{P}_\Lambda}$	268.0	8.2	21.4	15.3	11.6	8.7	10.1	7.7
$\chi^2_{\vec{P}_\Lambda}(90°)$	5.8	4.4	4.0	3.8	4.9	4.8	1.0	5.5
u channel $p(K^-,\gamma)\Lambda$								
Branching ratio (10^{-3})	1.79	0.96	0.28	4.32	14.38	0.97	0.90	1.03
expt.: $(0.86\pm0.17)\times10^{-3}$								

of Refs. 2–4.

Using a standard nonlinear χ^2-optimization routine,[9] we have found several parametrizations that simultaneously fit all the available angular distribution and Λ polarization data,[10] while predicting a branching ratio that is consistent with the recently published experimental value[11] of $(0.86\pm0.17)\times10^{-3}$ which is believed to be more accurate than the $(2.8\pm0.8)\times10^{-3}$ value reported by Lowe *et al.*[12] The new parameter sets are modified versions of those provided by previous researchers and, by and large, the numerical differences between new and old sets reflect the crossing constraint. Specifically, C1 and C2 are based on PR3a and PR4a, respectively. In Table II all parametrizations are compared by listing the values for the various couplings, the branching ratio they predict, along with the χ^2 per point for the cross section and polarization. The global χ^2_σ and $\chi^2_{P_\Lambda}$ per point include crossing section and Λ polarization data, respectively, for all available angles over the photon energy range from threshold to 1.4 GeV. The value of the total global χ^2 per point will be between χ^2_σ and $\chi^2_{P_\Lambda}$. Because of the large quantity of cross-section data near 1.2 GeV and polarization data at 90° we also show local χ^2 values for these kinematics as well. Throughout this paper the solid, dashed, dotted, and dotted-dashed curves represent C1, C2, PR4b, and PR5 sets, respectively. For comparison we also plot the curves for parameter set PR4b which is the best photoproduction fit, unconstrained by crossing, contained in Ref. 4. In Fig. 2(a) we present our first crossing result, the K^+ photoproduction cross section near threshold provided by sets C1, C2, PR4b, and PR5. It is important to note that curves C1, C2, and PR4b are fits whereas curve PR5, which exceeds the data by an order of magnitude, is a prediction based upon crossing a K^-p capture analysis. This sizable overprediction by the PR5 set is also present at higher energies and is not shown in subsequent figures [i.e., Figs. 2(b)–2(d)]. Using the parametrizations C1 and C2, we plot the pho-

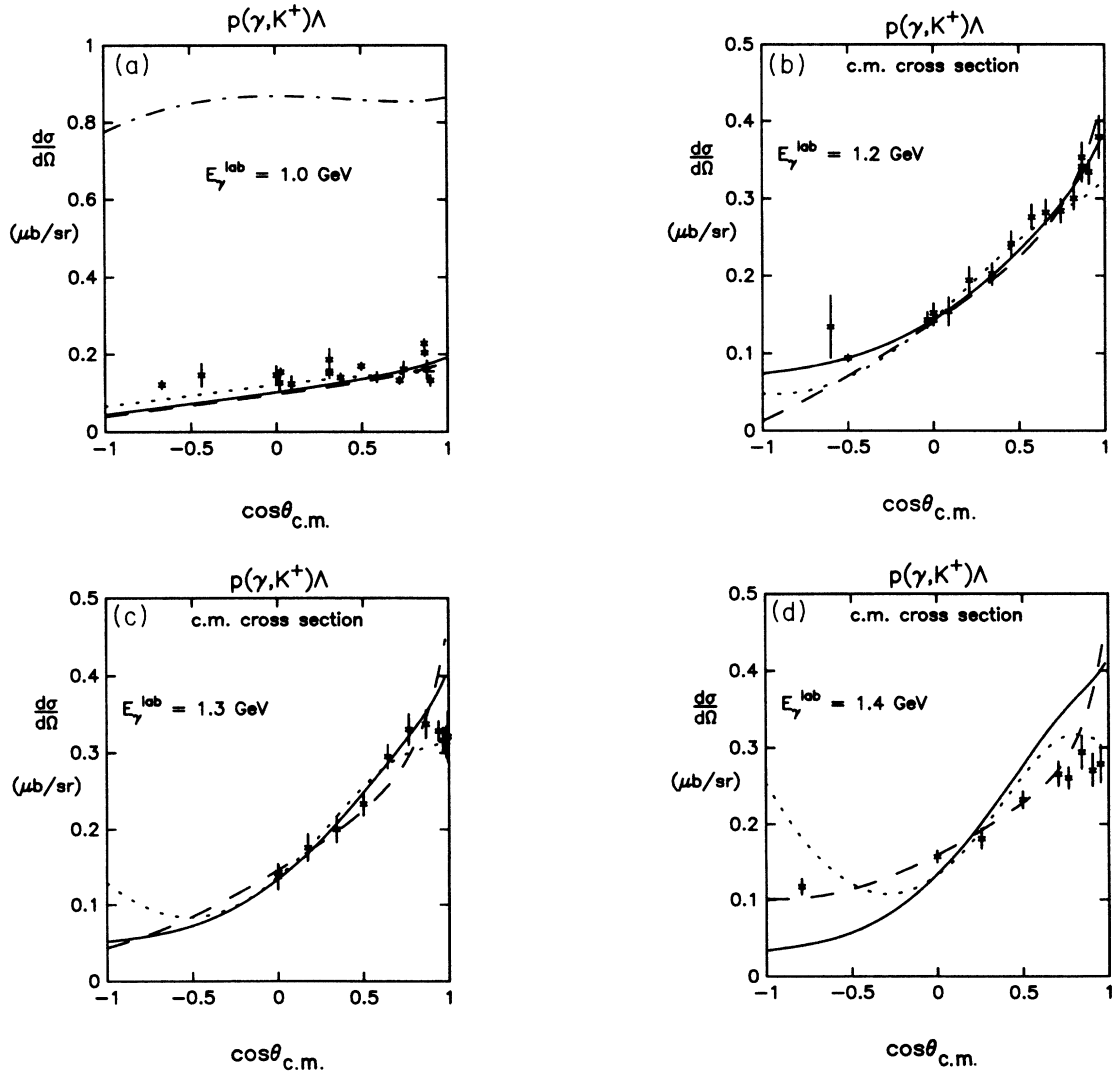

FIG. 2. Photoproduction cross-section predictions for C2 (dashed line), PR4b (dotted), and C1 (solid).

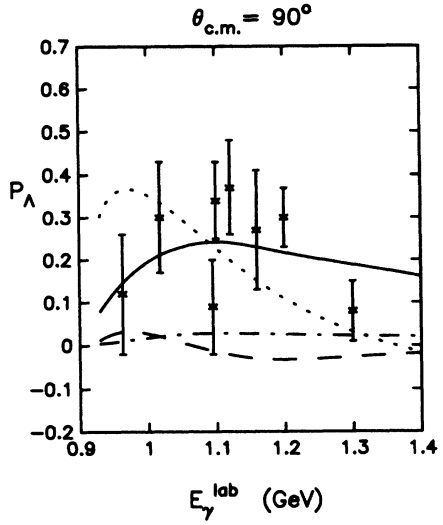

FIG. 3. Polarization curves with the same labeling as Fig. 2.

toproduction cross sections at 1.2, 1.3, and 1.4 GeV in Figs. 2(b)–2(d), and display Λ polarization curves at $\Theta_{\text{c.m.}}=90°$ in Fig. 3. Notice, that just as the PR5 set does not describe the production data well, the PR2, PR3b, and PR4(a,b) sets do not adequately reproduce the lambda channel K^-p decay width (see Table II). Set PR3a is consistent in both channels, but it contains only Born terms which are not capable of describing the polarization data.

We now discuss the key features of our crossing consistent parameter sets. Both sets provide a reasonable description of the data with χ^2 comparable to previously published fits. For the set C1 the magnitudes of $g_{K\Lambda N}$ and $g_{K\Sigma N}$ are within the rather wide range of values established by previous purely hadronic scattering analyses[13] although $g_{K\Lambda N}$ is somewhat smaller than that published by Martin[14] and $g_{K\Sigma N}$ is somewhat larger than the value reported by Antolin.[15] However, as discussed in Ref. 16, there exists a discrepancy between hadronic and electromagnetic analyses in determining g_{KYN} values. The parametrization C2 was constrained to provide larger $g_{K\Lambda N}$ and $g_{K\Sigma N}$ coupling constants to be more consistent with purely hadronic analyses. To achieve fits in this framework it was found necessary to increase the strength of certain resonance coupling parameters. This correlated enhancement of Born and resonant parameters was first reported in Ref. 4 and subsequently discussed in Ref. 6. However, our value for $g_{K\Sigma N}$ is again larger than that reported by Antolin.[15] We have searched but have been unsuccessful in finding a crossing consistent set that has a large $g_{K\Lambda N}$ and a small $g_{K\Sigma N}$.

Finally, we stress the importance of crossing as a way to systematically eliminate unphysical model parametrizations. Crossing produces a channel-dependent enhancement of a model's sensitivity to parameter uncertainties. Because the crossed diagrams are evaluated in a different kinematic region of the S matrix, the crossed diagrams will, in general, exhibit a different relative importance depending upon the channel. Hence, diagrams which are significant in one channel will not necessarily be significant in the crossed channel. This is certainly true when the coupling constants do not have any energy dependence as we have assumed in this analysis. This channel-dependent enhancement of a model's sensitivity to parameter uncertainties is a general feature of crossing which should be used to constrain and test all strong-coupling parametrizations. In general, phenomenological χ^2 parameter fits are not unique due to a large number of parameters which are usually not linearly independent. The χ^2 hypersurface will always have many local minima, and hence many phenomenological parametrizations can be found that do equally well fitting the data in one channel. However, these parametrizations will usually produce significantly different cross-channel predictions (due to enhancement/suppression effects), a very useful feature for selecting the optimal parameter set. To further demonstrate this point,[7] we display the $p(K^-,\gamma)\Lambda$ cross-section predictions for parameter sets C1, C2, PR4b, and PR5 in Fig. 4. Unfortunately, data for this reaction are

TABLE III. Q_{ij} Hermitian matrix elements used to evaluate the branching-ratio equation (3).

(i,j)	$\text{Re}Q^s_{ij}(s,t,u)$	$\text{Im}Q^s_{ij}(s,t,u)$
(1,1)	$(s-m_p^2)(u-m_p^2)$	0
(1,2)	$\frac{1}{2}[(s-m_p^2)^2m_\Lambda^2+(u-m_\Lambda^2)^2m_p^2-(s-m_p^2)(u-m_\Lambda^2)(t-m_p^2-m_\Lambda^2)]$	$m_p(u-m_\Lambda^2)+m_\Lambda(s-m_p^2)$
(1,3)	$\frac{1}{2}[(s-m_p^2)^2m_\Lambda-(s-m_p^2)(u-m_\Lambda^2)m_p]$	$(s-m_p^2)$
(1,4)	$\frac{1}{2}[(u-m_\Lambda^2)^2m_p-(s-m_p^2)(u-m_\Lambda^2)m_\Lambda]$	0
(2,2)	$-[t-(m_p-m_\Lambda)^2]\text{Re}Q^s_{1,2}(s,t,u)$	0
(2,3)	$-m_p\text{Re}Q^s_{1,2}(s,t,u)$	$\frac{1}{2}(m_p^2+m_\Lambda^2-t)(s-m_p^2)+m_p^2(u-m_\Lambda^2)$
(2,4)	$-m_\Lambda\text{Re}Q^s_{1,2}(s,t,u)$	$\frac{1}{2}(m_p^2+m_\Lambda^2-t)(u-m_\Lambda^2)+m_\Lambda^2(s-m_p^2)$
(3,3)	$\frac{1}{4}(s-m_p^2)^2[t-(m_p+m_\Lambda)^2]$	0
(3,4)	$-\frac{1}{4}[m_\Lambda(s-m_p^2)-m_p(u-m_\Lambda^2)]^2$	$\frac{1}{2}m_p(m_\Lambda^2-u)+\frac{1}{2}m_\Lambda(s-m_p^2)$
(4,4)	$\frac{1}{4}(u-m_\Lambda^2)^2[t-(m_p+m_\Lambda)^2]$	0

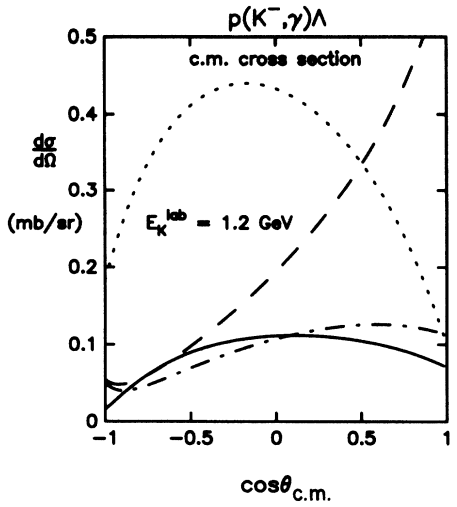

FIG. 4. Kaon-capture cross-section predictions with the same labeling as Fig. 2.

currently not available and we strongly recommend that this experiment be performed in the near future.

IV. CONCLUSIONS

Crossing has been used to develop several phenomenological strong-coupling parametrizations which simultaneously describe the kaon photoproduction and radiative capture reactions. By examining the parameter sets of previous researchers, who used the same effective Lagrangian model for these reactions but did not use the crossing constraint, we have shown how parametrizations that describe photoproduction well do not automatically describe the crossed-channel capture reaction adequately (and vice versa). Application of crossing was seen to produce a channel-dependent enhancement in the sensitivity to parameter uncertainties. This enhancement was seen to be useful for eliminating inconsistent sets of parameters.

It should be recognized, though, that imposing the fundamental crossing constraint is not sufficient to produce a unique set of parameters (especially in a large space such as C1 and C2). In part this is due to the limitations of the model and the questionable validity of an approach based upon a perturbative treatment of effective Lagrangians. Nevertheless, the thrust of this paper has been to demonstrate that crossing can be applied to enhance the utility and physical significance of phenomenologically determined coupling parameters. We stress that future investigations (both theoretical and experimental) must be performed before definitive conclusions can be reached on this model's validity including an unambiguous determination of coupling constants.

In conclusion, crossing is a powerful and useful constraint which can easily be applied to all phenomenological analyses where crossed-channel data exist. Similar analyses should be performed on other reactions where data are more accurate and abundant (e.g., pion photoproduction and capture, pion-nucleon, nucleon-nucleon scattering, etc.). We exhort the nuclear community to routinely incorporate crossing, both as a constraint on phenomenological studies, and as a stringent test in assessing the general validity and applicability of relativistic models.

ACKNOWLEDGMENTS

The authors acknowledge support provided by the U.S. Department of Energy under Contract No. DE-FG05-88ER40461.

APPENDIX

The elementary photoproduction amplitudes, $A_j^s(s,t,u)$, are obtained by the diagrammatic analysis of the graphs displayed in Fig. 1.

The amplitudes for the Born terms are given by

$$A_1^{\text{Born}} = \frac{g_\Lambda e}{s-m_p^2}(1+\kappa_p)+\frac{g_\Lambda e}{u-m_\Lambda^2}\kappa_\Lambda+\frac{G_\Sigma e}{u-m_\Sigma^2} + \frac{1}{t-m_{K^*}^2+im_{K^*}\Gamma_{K^*}}\left[\frac{G_\Lambda}{m}(m_\Lambda+m_p) + \frac{G_T t}{m(m_\Lambda+m_p)}\right],$$

$$A_2^{\text{Born}} = \frac{2g_\Lambda e}{(t-m_K^2)(s-m_p^2)} + \frac{1}{t-m_{K^*}^2+im_{K^*}\Gamma_{K^*}}\frac{G_T}{(m_p+m_\Lambda)m},$$

$$A_3^{\text{Born}} = \frac{g_\Lambda e}{(s-m_p^2)}\frac{\kappa_p}{m_p} + \frac{1}{t-m_{K^*}^2+im_{K^*}\Gamma_{K^*}}\left[\frac{G_V}{m}-\frac{G_T}{m}\frac{m_\Lambda-m_p}{m_\Lambda+m_p}\right],$$

$$A_4^{\text{Born}} = \frac{g_\Lambda e}{u-m_\Lambda^2}\frac{\kappa_\Lambda}{m_\Lambda}+\frac{2G_\Sigma e}{(u-m_\Sigma^2)(m_\Sigma+m_\Lambda)} + \frac{1}{t-m_{K^*}^2+im_{K^*}\Gamma_{K^*}}\left[\frac{G_V}{m}+\frac{G_T}{m}\frac{m_\Lambda-m_p}{m_\Lambda+m_p}\right],$$

where g_Λ, G_Σ, G_V, G_T are the effective couplings defined by Eqs. (7); s,t,u are the Mandlestam variables; κ_p,κ_Λ are the anomalous magnetic moments of the proton and lambda, respectively; m is an arbitrary mass (set equal to 1 GeV) inserted so that G_V and G_T are dimensionless.

The amplitudes for the s-channel N^* resonances can be written

$$A_1^{N(\frac{1}{2}^{\pm})}=\frac{G_{N^*}e(m_{N^*}\pm m_p)}{(s-m_{N^*}^2+im_{N^*}\Gamma_{N^*})(m_{N^*}+m_p)}\times\left[1-\frac{i\Gamma_{N^*}}{2(m_{N^*}+m_p)}\right],$$

$$A_2^{N(\frac{1}{2}^{\pm})}=0,$$

$$A_3^{N(\frac{1}{2}^{\pm})}=\frac{\pm 2G_{N^*}e}{(s-m_{N^*}^2+im_{N^*}\Gamma_{N^*})(m_{N^*}+m_p)},$$

$$A_4^{N(\frac{1}{2}^{\pm})}=0.$$

The amplitudes for the t-channel K_1 resonance are given by

$$A_1^{K_1}=0,$$

$$A_2^{K_1}=-\frac{G_T^{K_1}}{m(m_\Lambda+m_p)}\frac{1}{t-m_{K_1}^2+im_{K_1}\Gamma_{K_1}},$$

$$A_3^{K_1}=\frac{1}{t-m_{K_1}^2+im_{K_1}\Gamma_{K_1}}\left[\frac{G_V^{K_1}}{m}+\frac{G_T^{K_1}}{m}\frac{m_\Lambda-m_p}{m_\Lambda+m_p}\right],$$

$$A_4^{K_1}=-\frac{1}{t-m_{K_1}^2+im_{K_1}\Gamma_{K_1}}\left[\frac{G_V^{K_1}}{m}+\frac{G_T^{K_1}}{m}\frac{m_\Lambda-m_p}{m_\Lambda+m_p}\right].$$

The u-channel amplitudes of the Y^* resonances are given by

$$A_1^{Y(\frac{1}{2}^{\pm})}=\frac{G_{Y^*}e(m_{Y^*}\pm m_\Lambda)}{(u-m_{Y^*}^2+im_{Y^*}\Gamma_{Y^*})(m_{Y^*}+m_\Lambda)}\times\left[1-\frac{i\Gamma_{Y^*}}{2(m_{Y^*}+m_\Lambda)}\right],$$

$$A_2^{Y(\frac{1}{2}^{\pm})}=0,$$

$$A_3^{Y(\frac{1}{2}^{\pm})}=0,$$

$$A_4^{Y(\frac{1}{2}^{\pm})}=\frac{\pm 2G_{Y^*}e}{(u-m_{Y^*}^2+im_{Y^*}\Gamma_{Y^*})(m_{Y^*}+m_\Lambda)}.$$

The total amplitude is a sum of contributions from each diagram:

$$A_j^s(s,t,u)=A_j^{\text{Born}}(s,t,u)+\sum_{Y^*}A_j^{Y^*}(s,t,u)+\sum_{N^*}A_j^{N^*}(s,t,u)+A_j^{K_1}(s,t,u).$$

[1]We use QHD as a generic name for field theories with effective Lagrangians using only hadronic degrees of freedom. In the tree level, one can regard QHD as a pole model.

[2]H. Thom, Phys. Rev. **151**, 1322 (1966).

[3]R. A. Adelseck, C. Bennhold, and L. E. Wright, Phys. Rev. C **32**, 1681 (1985).

[4]R. A. Adelseck and L. E. Wright, Phys. Rev. C **38**, 1965 (1988); C. Bennhold and L. E. Wright, *ibid.* **39**, 927 (1989).

[5]R. L. Workman and Harold W. Fearing, Phys. Rev. D **37**, 3117 (1988).

[6]R. L. Workman, Phys. Rev. C **39**, 2076 (1989); R. A. Adelseck and L. E. Wright, *ibid.* **39**, 2078 (1989).

[7]Chueng-Ryong Ji and Stephen R. Cotanch, Phys. Rev. C **38**, 2691 (1988).

[8]H. Burkhardt, J. Lowe, and A. S. Rosenthal, Nucl. Phys. **A440**, 653 (1985).

[9]*Numerical Recipes: The Art of Scientific Computing,* edited by W. H. Press, B. R. Flannery, S. A. Teukolsky, and W. T. Vettering (Cambridge University Press, Cambridge, England, 1986). Subroutine MRQMIN p. 526.

[10]H. Genzel *et al.*, in *Photoproduction of Elementary Particles,* edited by H. Schopper (Landolt-Börnstein, Group I, Vol. 8) (Springer, Berlin, 1973).

[11]E. K. McIntyre *et al.*, in *Intersections Between Particle and Nuclear Physics,* proceedings of a conference, edited by Gerry M. Bunce (AIP Conf. Proc. No. 176) (AIP New York, 1988), p. 673; H. W. Fearing and R. L. Workman, *ibid.*, p. 677.

[12]J. Lowe *et al.*, Nucl. Phys. **B209**, 16 (1982); W. Humphreys and R. Ross, Phys. Rev. **127**, 1305 (1962).

[13]R. L. Warnock and G. Frye, Phys. Rev. **138**, B949 (1965); P. Baillon *et al.*, Phys. Lett. **50B**, 383 (1974); H. Pikhun *et al.*, Nucl. Phys. **B65**, 460 (1975).

[14]A. D. Martin, Nucl. Phys. **B179**, 33 (1981).

[15]J. Antolin, Phys. Rev. D **35**, 122 (1987).

[16]J. Cohen, Phys. Lett. **153B**, 367 (1985); Phys. Rev. C **39**, 2285 (1989).